Single-crystal IR- and UV/VIS-spectroscopic measurements on transition-metal-bearing pyrope: The incorporation of hydroxide in garnet

Article *in* European Journal of Mineralogy · March 2000

DOI: 10.1127/0935-1221/2000/0012-0259

CITATIONS
37

READS
610

3 authors, including:

Charles A. Geiger
University of Salzburg
240 PUBLICATIONS **4,207** CITATIONS

SEE PROFILE

Eur. J. Mineral.
2000, **12**, 259-271

Single-crystal IR- and UV/VIS-spectroscopic measurements on transition-metal-bearing pyrope: the incorporation of hydroxide in garnet

CHARLES A. GEIGER[1,*], ANDREAS STAHL[1] and GEORGE R. ROSSMAN[2]

[1]Institut für Geowissenschaften der Christian-Albrechts-Universität zu Kiel, Olshausenstraße 40, D-24098 Kiel, Germany

[2]California Institute of Technology, Division of Geological and Planetary Sciences, Pasadena, CA 91125, U.S.A.

Abstract: Pyrope single crystals doped with transition-metal ions (Co, Cr, Ni, Ti and V) were synthesised in a piston-cylinder device at 950-1050°C and 25 kbar. Stoichiometric oxide mixtures were used as starting materials and distilled water was used as a fluid flux. Crystals up to 2 mm in size were grown. Microprobe analysis and optical absorption spectroscopy were used to determine on which positions and in which oxidation states the transition-metal ions are incorporated in the pyrope structure. Cr^{3+}-ions occupy the octahedral site and Co^{2+} and Ni^{2+} the dodecahedral site. Although extra metallic Ti was included in the synthesis of Ti-bearing pyropes, only Ti^{4+} and no measurable Ti^{3+} could be stabilised on the octahedral site. The optical absorption spectra of V-bearing pyropes show, in addition to the spin-allowed dd-transitions $^3T_{1g}(F) \rightarrow {}^3T_{2g}(F)$ at ~ 17000 cm^{-1} and $^3T_{1g}(F) \rightarrow {}^3T_{1g}(P)$ at ~ 20000 cm^{-1} corresponding to V^{3+} on the octahedral site, absorption bands which are thought to be caused by dd-transitions of V^{3+} in the tetrahedral site and V^{4+} on octahedral and tetrahedral sites. V^{4+} was not observed in silicate garnets before. IR spectra in the OH^- stretching region between 4000 and 3000 cm^{-1}, obtained on pyrope single-crystals which only contain divalent and trivalent transition-metal ions like Ni^{2+}, Co^{2+}, and Cr^{3+}, are similar to that normally shown by end-member pyrope (Geiger *et al.*, 1991). At room temperature the spectra show a single band at ≈ 3630 cm^{-1}, which splits at ~79 K into two bands of smaller FWHM's at ≈ 3618 cm^{-1} and 3636 cm^{-1}. These bands are assigned to OH^--stretching modes resulting from the hydrogarnet substitution. The spectra of Ti^{4+}-bearing pyrope measured at 298 K show four OH^--stretching bands at approximately 3686, 3630, 3567 and 3527 cm^{-1}. At ~79 K the band at 3630 cm^{-1} splits into two narrow bands at 3636 cm^{-1} and 3614 cm^{-1}. This suggests that additional OH^- substitutional mechanisms occur in Ti-containing garnets. In the IR spectrum of a V^{4+}-bearing pyrope the same number of OH^-–stretching bands is observed, suggesting that higher charged cations cause additional OH^- substitutions and increased OH^- concentrations in garnet. The IR spectra of most natural pyrope-rich garnets appear to be different from those of the synthetics, which suggests that they are not characterised by the hydrogarnet substitution. However, the OH^-–substitution mechanism and concentrations in garnets from grospydite or similar parageneses are similar to those of the synthetics, which may reflect their formation in water-rich environments.

Key-words: UV/VIS and IR absorption spectroscopy, transition-metal ions, pyrope, OH^-–groups, hydrogarnet substitution, grospydites.

Introduction

The question of the bulk-water content of Earth's mantle and its influence on petrological and geophysical processes is of fundamental geological importance. However, it is not clear how much water is present or in what form at the pressures and temperatures of Earth's interior. It has

*e-mail: NMP46@rz.uni-kiel.de

DOI: 10.1127/0935-1221/2000/0012-0259 $ 3.25

been shown that small or trace amounts of OH^- (loosely referred to as water) are located in nominally anhydrous minerals (*e.g.* Martin & Donnay, 1972; Wilkins & Sabine, 1973; Bell & Rossman, 1992b), where it can influence both geophysical and geochemical processes. Since garnet is one of the important minerals of the upper mantle and transition zone, much work has been done to investigate the incorporation of a hydrous component into its structure (*e.g.* Ackermann *et al*., 1983; Aines & Rossman, 1984; Rossman *et al.*, 1989; Geiger *et al.*, 1991; Bell & Rossman, 1992a; Khomenko *et al.*, 1994a; Withers *et al.*, 1998; Matsyuk *et al.*, 1998). The only experimentally substantiated substitution mechanism for the incorporation of OH^- groups in garnet, although others must exist, is the hydrogarnet substitution, which is the exchange of one Si^{4+} cation by four H^+, leading to the formation of $(OH)_4^{4-}$ clusters (*e.g.* Cohen-Addad *et al.*, 1967; Lager *et al.*, 1989). Detailed structural information relating to this substitution in katoite ($Ca_3Al_2[O_4H_4]_3$) and in katoite-grossular solid solutions is given by Lager *et al.* (1989). Based on the symmetry of $(OH)_4^{4-}$ clusters, two OH^--stretching bands occur in the MIR spectra of such garnets (Harmon *et al.*, 1982). For the complicated "multi-band" spectra of some natural garnets (Rossman *et al.*, 1989), other OH^--substitution mechanisms than the hydrogarnet substitution have been proposed, but never substantiated. On the basis of X-ray diffraction studies, Basso *et al.* (1984) proposed more general substitutions in which protons substitute for cations not only on the tetrahedral, but also on the octahedral and dodecahedral sites. Cho & Rossman (1993) showed in a solid-state proton NMR study on grossular that, besides four proton clusters, two proton clusters can also be identified. Khomenko *et al.* (1994a) argued that the substitution of Ti^{4+} for Al^{3+} on the octahedral site in pyrope is coupled with the incorporation of OH^- groups on the tetrahedral site in the form of $[O(OH)_3]^{5-}$ clusters.

Some studies have also investigated the role of garnet composition on the resulting IR spectra, but only in the case of natural garnets (Bell & Rossman, 1992a; Matsyuk *et al.*, 1998). Little is understood with regard to the question of garnet chemistry and the type and number of OH^- absorption band(s) which have been observed. The problem is difficult to address, because the concentrations of OH^- are typically very low and because natural garnets are compositionally complex and have usually experienced a complex P-T history. The best way to address these questions is to undertake experimental studies in the laboratory, because garnet crystals of well-defined composition can be synthesised under controlled pressure and temperature conditions.

We used this experimental approach herein. To begin, we synthesised pyrope-rich garnets containing small concentrations of various transition metal cations (*i.e.* Co, Ni, *etc.*) at high pressure and high temperature under water-saturated conditions. We characterised these pyropes with electron microprobe analyses and UV/VIS absorption spectroscopy to determine the site substitution and valency of the different cations. Finally, we studied the single crystals by IR methods to discern the OH^- substitution mechanism(s) and to determine the OH^- concentrations. Withers *et al.* (1998) have shown that the OH^- contents in hydrothermally synthesised end-member pyrope begin to decrease at pressures around 6 GPa. It remains to be explored, though, what effect the incorporation of various transition-metal cations have on OH^--concentrations. We have focused our attention on pyrope-rich garnets for two reasons. First, they tend to show the simplest IR spectra of the silicate garnets. Second, petrologically important high-pressure garnets of the upper mantle are pyropic in composition.

Experimental methods

Synthesis

A number of different pyrope-rich compositions were prepared using various oxide mixtures. The oxides used in the synthesis experiments are the following: Al_2O_3 (Heraeus, 99.99 %), CoO (Johnson Matthey, 95 %), Cr_2O_3 (Johnson Matthey, 99.997 %), MgO (Heraeus, 99.99 %), NiO (Johnson Matthey, 99.998 %), SiO_2 (Chempur, 99.99 %), Ti_2O_3 (Johnson Matthey, 99 %), and V_2O_5 (Johnson Matthey, 95 %). We started by preparing an oxide mixture of pyrope composition ($3MgO, Al_2O_3, 3SiO_2$). Different garnet compositions were also prepared containing various transition metal ions which were to be incorporated into pyrope-rich solid solutions. For the preparation of the final compositions, we combined together certain percentages of the pyrope mix together with a transition-metal-containing mix (Table 1). The solid-solution compositions consisted generally of 3 to 10 mole % of the transition-metal garnet component and 90 to 97 mole % pyrope component. The oxides MgO, Al_2O_3 and SiO_2, prior to weighing, were fired in Pt

crucibles at 1000°C for a minimum of 10 hours to remove adsorbed water and any combustible contaminants. The transition-metal oxides were dried for at least 12 hours, but only at 120°C to avoid oxidation. The homogeneity of the starting mixes was ensured by grinding them intimately under distilled H_2O in an agate mortar for about two hours and examining the mix under a binocular microscope. Both the oxides and their mixtures were stored in a desiccator prior to synthesis.

The single-crystal syntheses were undertaken using a piston-cylinder device. 100-150 mg of oxide mix and 5-7 µl of doubly distilled H_2O, used as the fluid flux, were added to Au capsules with outer dimensions of 5 mm diameter and 8 mm length and with a wall thickness of about 0.5 mm. Different oxidising or reducing agents were added to the capsules in some cases in order to fix or direct the oxidation state of the transition metals during synthesis (Table 1). The capsules were sealed and placed in a 19.05 mm diameter salt assembly as described in Cemič *et al*. (1990). The synthesis conditions and durations of the experiments are given in Table 1. The P-T conditions were chosen to produce large single crystals (Geiger *et al.*, 1991). A total of about 30 experiments were undertaken of which about half are reported herein. After a run, the capsules were checked to see that they remained tight and that water was present during garnet growth.

Characterisation

Microprobe analysis

The composition and chemical homogeneity of the garnet crystals were characterised by electron-microprobe analysis using a Camebax microprobe. The beam size was 1 µm in diameter with an accelerating voltage of 15 kV and a beam current of 15 nA. For each measurement, 20 s count-

Table 1. Composition of the starting materials and synthesis conditions.

Sample label	Composition of the oxide mixture [mole %]	P [kbar]	T [°C]	Duration [h]	Other phases*
B006	97 % $Mg_3Al_2Si_3O_{12}$ 3 % $Mg_3Cr_2Si_3O_{12}$	25	1050	18	-
K007	97 % $Mg_3Al_2Si_3O_{12}$ 3 % $Ni_3Al_2Si_3O_{12}$	25	950	17	-
B008	97 % $Mg_3Al_2Si_3O_{12}$ 3 % $Mg_3V_2Si_3O_{12}$	25	1050	18	-
K017	97 % $Mg_3Al_2Si_3O_{12}$ 3 % $Mg_3V_2Si_3O_{12}$	25	950	17	V
K020	90 % $Mg_3Al_2Si_3O_{12}$ 10 % $Mg_3V_2Si_3O_{12}$	25	950	18	-
K021	96 % $Mg_3Al_2Si_3O_{12}$ 3 % $Mg_3V_2Si_3O_{12}$ 1 % $Mg_3Ti_2Si_3O_{12}$	25	950	20	-
K012	97 % $Mg_3Al_2Si_3O_{12}$ 3 % $Mg_3Ti_2Si_3O_{12}$	25	950	17	Ti
P001	97 % $Mg_3Al_2Si_3O_{12}$ 3 % $Mg_3Ti_2Si_3O_{12}$	25	990	22	Ti
K016	97 % $Mg_3Al_2Si_3O_{12}$ 3 % $Mg_3Ti_2Si_3O_{12}$	25	950	20	-
K008	98 % $Mg_3Al_2Si_3O_{12}$ 2 % $Mg_3Ti_2Si_3O_{12}$	25	950	17	-
K005	97 % $Mg_3Al_2Si_3O_{12}$ 3 % $Co_3Al_2Si_3O_{12}$	25	950	17	-
K018a	80 % $Mg_3Al_2Si_3O_{12}$ 20 % $Co_3Al_2Si_3O_{12}$	25	950	16	-
K018b	60 % $Mg_3Al_2Si_3O_{12}$ 40 % $Co_3Al_2Si_3O_{12}$	25	950	17	-
K018c	40 % $Mg_3Al_2Si_3O_{12}$ 60 % $Co_3Al_2Si_3O_{12}$	25	950	20	-
K018d	20 % $Mg_3Al_2Si_3O_{12}$ 80 % $Co_3Al_2Si_3O_{12}$	25	950	16	-
KG001	100% $Co_3Al_2Si_3O_{12}$	25	950	17	-

* used to buffer or to act as a reduction or oxidizing agent.

ing time was used on the peak centre and for the background 10 s on each side of the peak. The following standards were used: MgO for Mg, Al_2O_3 for Al, natural wollastonite for Si and Ca, Co for Co, Ni for Ni, V for V, Cr_2O_3 for Cr, TiO_2 for Ti. The data correction program employed was supplied by Cameca and is entitled PAP (Pouchoux & Pichoire). Line scans were made to check for compositional zonation.

Optical absorption spectroscopy

For the optical absorption spectroscopic measurements, doubly polished plates of varying thickness were prepared from the single crystals. Measurements were made at the California Institute of Technology using a home-made diode array microscope spectrometer in the UV and visible region (VIS) and a Nicolet 60SX FT-IR spectrometer in the NIR and MIR region. The beam size was selected to be between 20 and 100 μm in diameter. The spectra were recorded in different wavelength regions and then merged to give the final spectrum between approximately 40000-5000 cm^{-1}. The spectral resolution was 4 cm^{-1} in the infrared and 1 nm in the VIS and UV range. A Si detector and SiO_2 beamsplitter with either a Xe or W source were used for the measurements. Between 48 and 1024 scans were collected for each spectrum.

IR spectroscopy

Measurements in the wavenumber region between 4000 and 3000 cm^{-1} were undertaken at Kiel on the same crystal platelets with a Bruker IFS 66V/S FT-IR spectrometer equipped with an infrared microscope. A HgCdTe detector, a KBr beamsplitter and a SiC source were used in the measurements. The spectral resolution was 4 cm^{-1} and the beam diameter was adjusted to account for the crystal size and the inclusion density and varied between 20–50 μm. Low-temperature measurements (~79 K) were undertaken using a HSF 91 Linkam cooling system. For quantitative evaluation of the OH^- bands, integrated intensities were determined as sums of all intrinsic OH^- bands using the program Origin 3.73 with a peak fitting module (Microcal Software, Inc.).

Results

Synthesis results

Syntheses often produced large single crystals up to 1-2 mm in size. The results are summarised in Table 2. We were not successful in growing large single crystals with Mn^{2+} or Fe^{2+} on the dodecahedral site. Such synthesis experiments are not described herein. Many syntheses resulted in the growth of better than 95 % garnet, but in some cases additional phases, normally occurring as fine-grained material, were identified. The experiments herein were not made with excess SiO_2, but this is not considered to have an effect on the substitutional mechanism or the OH^- concentrations (see Geiger *et al.*, 1991). The synthetic pyrope-rich crystals are generally euhedral and show well developed {110} and sometimes {211} faces. The colour of the crystals varies greatly reflecting the incorporation of the different transition-metal cations. Chromium- and Ni-bearing pyropes are light pink to red, Co-bearing pyropes are light to dark violet-red, depending on their Co concentration, V-bearing pyropes are dark greenish blue and the Ti-bearing pyropes are colourless. Single crystals generally contain small inclusions, which consist of H_2O and/or unreacted or partially reacted starting materials. The Co- and Ni-bearing pyropes contain small inclusions of Co-spinel or Ni-spinel identified through microprobe analyses. The inclusion density increases from the rim to the centre of the crystals (Geiger *et al.*, 1991). Inclusion-free regions on the rims are large enough to measure UV/VIS and IR spectra without interference from the inclusions.

Microprobe analysis

Structural formulae determined from the

Table 2. Description of the synthetic crystals.

Sample	Color	Diameter (mm)	Observed forms	Inclusions
Cr-Pyrope	pinkish-red	1.0-1.5	{110}	water
Ni-Pyrope	pink	1.0-1.5	{110}	water, Ni-Spinel
V-Pyrope	greenish-blue	1.0-1.5	{110}&{211}	water
Ti-Pyrope	colourless	1.0-3.0	-	water
Co-Pyrope	violet-red	0.5-1.0	{110}	water, Co-Spinel

Table 3. Microprobe analyses of the single crystals.

Sample label	Cations per Formula Unit on a 12-oxygen basis					Sum	Number of data points
	Mg	**Al**	**Si**	**Cr^{3+}**			
B006	2.98(5)	1.93(3)	3.03(3)	0.04(4)		7.98(2)	27
	Mg	**Al**	**Si**	**Ni**			
K007	2.98(4)	1.98(8)	3.01(6)	0.03(2)		8.00(3)	40
	Mg	**Al**	**Si**	**V^{3+}**	**Ti^{4+}**		
B008	3.00(6)	1.93(3)	3.01(3)	0.06(3)	-	8.00(3)	40
K017	2.98(3)	1.85(4)	3.02(2)	0.13(4)	-	7.99(1)	39
K020	2.97(2)	1.83(1)	3.01(2)	0.17(2)	-	7.99(1)	23
K021	2.97(2)	1.89(1)	3.02(1)	0.06(1)	0.03(1)	7.97(2)	10
	Mg	**Al**	**Si**	**Ti^{4+}**			
K012	3.01(2)	1.93(2)	3.00(2)	0.04(1)		7.99(1)	29
P001	3.03(2)	1.95(2)	2.98(1)	0.04(1)		8.00(1)	28
K016	2.99(3)	1.95(2)	3.00(3)	0.05(1)		7.98(2)	19
K008	2.99(3)	1.94(3)	3.02(2)	0.03(2)		7.98(2)	40
	Mg	**Al**	**Si**	**Co**			
K005	2.90(4)	1.97(2)	3.02(2)	0.10(4)		7.99(2)	41
K018a	2.47(3)	2.01(1)	2.98(1)	0.56(2)		8.02(1)	14
K018b	1.69(3)	2.03(2)	2.97(1)	1.32(4)		8.01(1)	15
K018c	1.15(9)	1.98(2)	3.01(2)	1.86(8)		8.00(2)	16
K018d	0.70(3)	2.01(2)	2.97(2)	2.34(2)		8.02(1)	15
KG001	-	1.98(2)	2.99(2)	3.04(4)		8.01(2)	12

microprobe analyses are listed in Table 3 (a list of the oxide wt. percentages for analyses made on the different garnets can be obtained from the first author upon request). We found no evidence for compositional zonation in individual crystals. Any variations from garnet stoichiometry are probably experimental artefacts (resulting from inclusions, cracks, *etc.*) and do not reflect compositional deviations. Therefore, all point analyses were averaged. It was not always possible to determine unambiguously where the transition-metal ions are structurally incorporated on the basis of the calculated structural formulae, because their concentrations are low. Moreover, it is possible in some cases that they occur in different oxidation states, which can not be easily measured by electron microprobe techniques. Here optical absorption spectroscopy must be employed.

Optical absorption spectra

The single-crystal optical absorption spectra of the different pyrope-rich garnets, normalised to 1 cm thickness, are shown in Fig. 1 to 4. In order to determine where in the garnet structure the different transition metal cations are incorporated, literature data, together with Tanabe-Sugano diagrams (Tanabe & Sugano, 1954) were used.

The spectrum of Cr^{3+}-bearing pyrope (B006) shows two broad bands at 18000 and 24500 cm^{-1} (Fig. 1). For a $3d^3$-ion in ideal octahedral coordination, three spin-allowed transitions from the ground state $^4A_{2g}(^4F)$ are predicted. They are $^4A_{2g}(^4F) \rightarrow {}^4T_{2g}(^4F)$, $^4A_{2g}(^4F) \rightarrow {}^4T_{1g}(^4F)$, and $^4A_{2g}(^4F) \rightarrow {}^4T_{1g}(^4P)$. The bands at 18000 and 24500 cm^{-1} are assigned to the first two spin-allowed transitions (Amthauer, 1976). The third spin-allowed band occurs in the UV region where it is hidden under a ligand-metal charge-transfer band, which is significantly higher in intensity. Spin-forbidden bands are not observed, because of the low Cr^{3+} concentration.

The theoretical group labels for Co^{2+} ($3d^7$-ion) occurring in an ideal eightfold coordinated cubic environment and octahedral Cr^{3+} are identical and the same number of dd-transitions may appear [$3d^3$(oct.) ≡ $3d^7$(cubic) - Burns, 1993]. The spectrum of end-member $Co_3Al_2Si_3O_{12}$ (KG001) shows three band envelopes centred at approximately 4333, 8079 and 18361 cm^{-1} (Fig. 2). They correspond to transitions from the ground state, $^4A_{2g}(^4F)$, to the three spin-allowed excited states $^4T_{2g}(^4F)$, $^4T_{1g}(^4F)$ and $^4T_{1g}(^4P)$, respectively (Ross *et al.*, 1996). Splitting within these three major absorption envelopes results from a lifting of the degeneracy due to the orthorhombic distortion of the dodecahedral site. Moreover, in the highest-energy envelope splitting due to spin-orbit coupling or contributions from strong intensity enhanced spin-forbidden transitions is also occurring. Pyrope-rich cobalt-poor garnets (*i.e.* $Mg_{2.9}Co_{0.1}Al_2Si_3O_{12}$ – sample K005) show similar

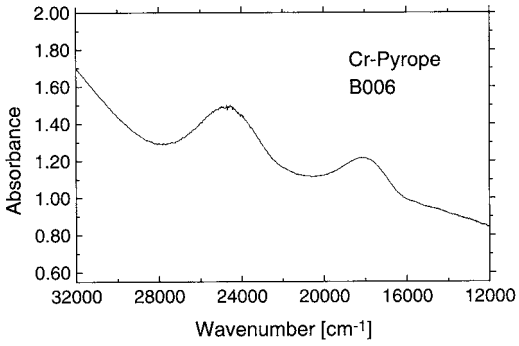

Fig. 1. Crystal-field spectrum of Cr-bearing pyrope B006.

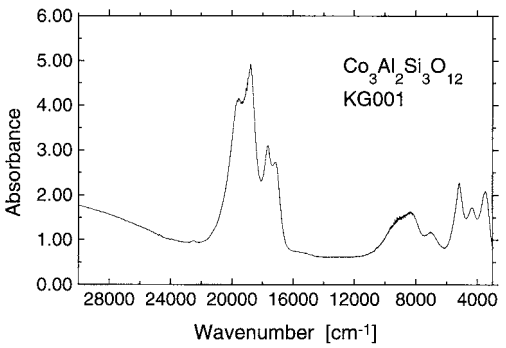

Fig. 2. Crystal-field spectrum of $Co_3Al_2Si_3O_{12}$ KG001.

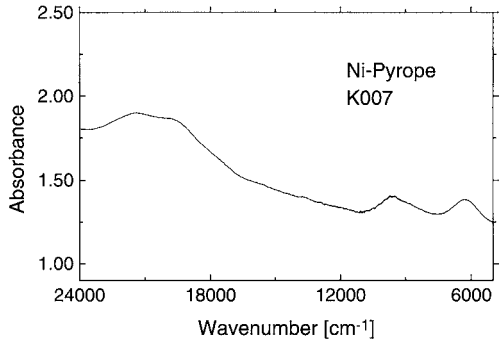

Fig. 3. Crystal-field spectrum of Ni-bearing pyrope K007.

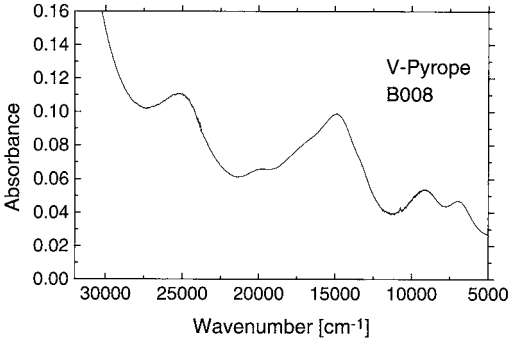

Fig. 4. Crystal-field spectrum of V-bearing pyrope B008.

spectra as end-member Co-garnet, except that the bands are shifted slightly to higher wavenumbers. This shift could be caused by stronger crystal fields acting on the Co^{2+}-ions at lower concentrations. Spin-forbidden bands may be present around 23000 cm^{-1}, but are difficult to ascertain with complete certainty.

The spectrum of Ni-bearing pyrope ($(Mg_{0.99}Ni_{0.01})_3Al_2Si_3O_{12}$ – sample K007) is shown in Fig. 3. The spectrum consists of a split band located at 20842 cm^{-1} and two bands in the NIR region at 9553 and 6313 cm^{-1}. The spectrum of a pyrope with a higher Ni-content ($(Mg_{0.82}Ni_{0.18})_3Al_2Si_3O_{12}$), measured by Ross *et al.* (1996), also shows two transitions in the NIR-region, which, however, are located at lower energies of 6210 and 4070 cm^{-1}. At higher energies a split band is observed at 20640 cm^{-1}. The ground state of Ni^{2+} in an ideal eightfold-coordinated cubic environment is $^3T_{1g}(^3F)$. The three bands are assigned to the three spin-allowed transitions from the ground state to $^3T_{2g}(^3F)$, $^3A_{2g}(^3F)$ and $^3T_{1g}(^3P)$ with increasing wavenumbers, respectively. Although the site symmetry of the Ni^{2+} cation is orthorhombic, the dd-bands are not as greatly split as in the case of Co-bearing garnet (Fig. 2). The reason for this is not understood. Ross *et al.* (1996) showed that, although the Ni^{2+}-ionic radius is smaller than that of Mg^{2+}, the pyrope structure opens up with increasing Ni concentration. The shift of the bands to higher wavenumbers in the spectrum of our Ni-bearing pyrope, as compared to those in the garnet of Ross *et al.* (1996), might be a result of such changes in the garnet structure. However, the expected energy ratio of the transitions $^3T_{1g}(^3F) \rightarrow {}^3T_{2g}(^3F)$ and $^3T_{1g}(^3F) \rightarrow {}^3A_{2g}(^3F)$ is not in agreement with that predicted by the Tanabe-Sugano diagram for a $3d^8$-ion in ideal eightfold coordination and this assignment can not be made with complete confidence. Spin-forbidden bands are difficult to observe except for a possible band around 13500 cm^{-1}.

The V-bearing pyropes show the most complicated spectra. A typical spectrum is that of V-bearing pyrope B008 (Fig. 4). Bands are located at

approximately 24824, 20607, 16566, 14590, 13038, 9133 and 6855 cm^{-1}. The crystal-field spectra of natural garnets containing V^{3+} on the octahedral site show two dd-transitions. They are located at 17600-16000 cm^{-1} and 24500-22500 cm^{-1} depending on composition (Schmetzer & Ottemann, 1979). They are assigned to the spin-allowed transitions $^3T_{1g}(^3F) \rightarrow {}^3T_{2g}(^3F)$ and $^3T_{1g}(^3F) \rightarrow {}^3T_{1g}(^3P)$. A comparison of our spectra with the spectra of V^{3+}- and V^{4+}-doped yttrium aluminium garnet (Weber & Riseberg, 1971) suggests that not only V^{3+} is present, but also V^{4+}. The spectrum of the V-doped YAG's show seven dd-transitions having band energies similar to our synthetic V-bearing pyrope, except that each is shifted to slightly higher wavenumbers. Therefore, in sample B008 the transitions at 24824 and 16566 cm^{-1} are assigned to V^{3+} in octahedral coordination, all others, except for the transitions in the NIR region, to V^{4+} in either octahedral (20607 $cm^{-1} \triangleq {}^2T_{2g}(^2D) \rightarrow {}^2E_g(^2D)$) or tetrahedral (14590 and 13038 $cm^{-1} \triangleq$ split $^2E_g(^2D) \rightarrow {}^2T_{2g}(^2D)$) coordination (Weber & Riseberg, 1971). The transitions in the NIR region of V-doped YAG could not be satisfactory assigned by Weber & Riseberg (1971). They suggest that they result from V^{2+} in dodecahedral or V^{3+} in tetrahedral coordination. We believe that the first case is improbable, because the presence of V^{4+} suggests oxidising conditions during crystal growth. Our assignments, however, have to be treated carefully, because no spectra showing V^{4+} in silicate garnets are available for comparison. The V^{3+}/V^{4+} ratio in the V-pyropes is difficult to quantify, but based on the integrated intensities of the bands and considering the Laporte selection rule, it is probable that

Table 4. Peak positions and full width at half-maximum height (FWHM) at 298 K (RT) and 79 K (LN) and calculated water contents of the synthesised garnets.

Sample	A [cm^{-2}]	c_{H_2O}* [wt. %]		Peak positions and (FWHM) at 298 K (RT) und 79 K (LN) [cm^{-1}]			
Cr-Pyrope (B006)	440	0.03	RT	3627 (50)	-	-	-
			LN	3638 (11) 3613 (16)	-	-	-
Ni-Pyrope (K007)	480	0.03	RT	3629 (66)	-	-	-
			LN	3638 (11) 3613 (16)			
Co-Pyrope (KG001)	-	-	RT	3624 (64)			
V-Pyrope (B008)	230	0.02	RT	3630 (66)	-	-	-
			LN	3639 (12) 3615 (16)	-	-	-
V-Pyrope (K017)	700	0.05	RT	3663 (22)	3632 (27) 3616 (18)	3587 (21)	3520 (52)
			LN	3674 (11)	3639 (12) 3619 (19)	3584 (16)	3519 (29)
V-Pyrope (K020)	109	0.01	RT	3629 (52)	-	-	-
V,Ti-Pyrope (K021)	800	0.06	RT	3685 (15)	3629 (66)	3568 (26)	3527 (43)
			LN	3696 (12)	3640 (15) 3612 (47)	3566 (26)	3523 (24)
Ti-Pyrope (K012)	760	0.05	RT	3686 (15)	3630 (70)	3567 (23)	3527 (34)
			LN	3697 (12)	3639 (12) 3611 (20)	3565 (18)	3520 (27)
Ti-Pyrope (P001)	590	0.04	RT	3686 (16)	3628 (65)	3567 (26)	3527 (42)
Ti-Pyrope (K016)	610	0.04	RT	3686 (16)	3630 (64)	3566 (24)	3526 (37)
Ti-Pyrope (K008)	646	0.05	RT	3686 (16)	3631 (66)	3567 (24)	3526 (37)

* after Bell & Rossman (1992a)

the V^{3+} concentration is significantly higher than that of V^{4+}.

All our Ti-bearing pyropes show no absorption bands in their UV/VIS and NIR spectra. Ti-rich andradite-rich garnets show one dd-electronic band which Manning & Harris (1970) proposed indicated Ti^{3+} on the octahedral site. However, if Ti^{3+} was incorporated in pyrope, one spin-allowed transition ($^2T_{2g}(^2D) \rightarrow {}^2E_g(^2D)$), with two components due to Jahn-Teller splitting, should be present at approximately 16000-20000 cm^{-1} (Khomenko *et al.*, 1994b). Therefore, it is proposed that titanium enters the pyrope structure in its tetravalent state in our garnets, since no dd-transitions are observed. Microprobe analyses show that titanium substitutes for aluminium on the octahedral site. However, it can not be excluded that Ti^{4+} also enters the tetrahedral site in small amounts (Reid *et al.*, 1976). In the case of andradite, it has been shown that Ti^{4+} prefers the octahedral site, but can also replace Si^{4+} on the tetrahedral site (Armbruster *et al.*, 1998).

IR spectroscopy

Single-crystal IR spectra of the different transition-metal containing pyropes are shown in Fig. 5-13. All spectra are normalised to a sample thickness of 1 cm to allow easy comparison. The band maxima and integrated intensities and the estimated water concentrations are listed in Table 4. The water contents were calculated after Bell & Rossman (1992a).

The room-temperature spectra of pyrope containing trivalent and divalent transition metal ions such as Cr^{3+}, Co^{2+} and Ni^{2+} (B006, K005, K007) show a single OH^- absorption band located at approximately 3630 cm^{-1} (Fig. 5, 6, and 7). In the spectra of garnets with high Co concentrations

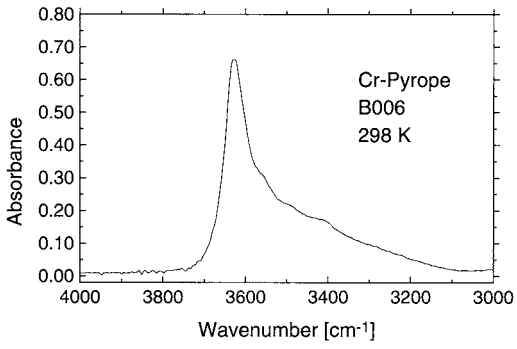

Fig. 5. MIR spectrum of Cr^{3+}-bearing pyrope B006 at 298 K.

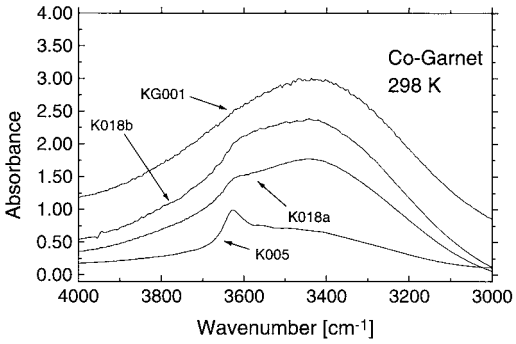

Fig. 6. Comparison of the MIR spectra of the $(Co,Mg)_3Al_2Si_3O_{12}$ garnets at 298 K.

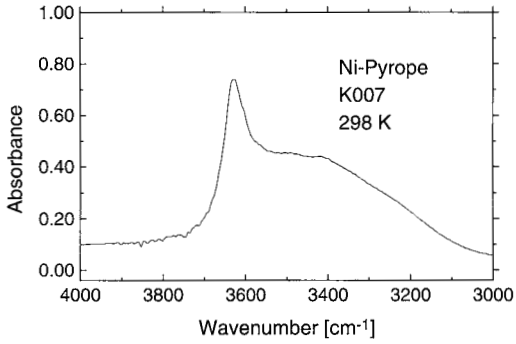

Fig. 7. MIR spectrum of Ni^{2+}-bearing pyrope K007 at 298 K.

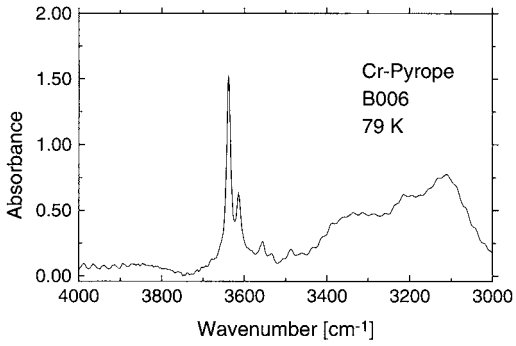

Fig. 8. MIR spectrum of Cr^{3+}-bearing pyrope B006 at 79 K.

(K018a-b and KG001), this band is obscured by a broad dd-transition band centred at approximately 3450 cm^{-1} (Fig. 6). At ~79 K the OH^- band splits into two bands centred at approximately 3636 and 3614 cm^{-1} (Fig. 8 for Cr-bearing pyrope). In contrast, the Ti^{4+}-bearing pyropes show more than two absorption bands. Four bands are observed at

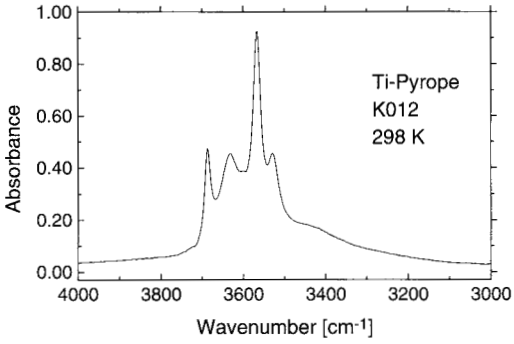

Fig. 9. MIR spectrum of Ti^{4+}-bearing pyrope K012 at 298 K.

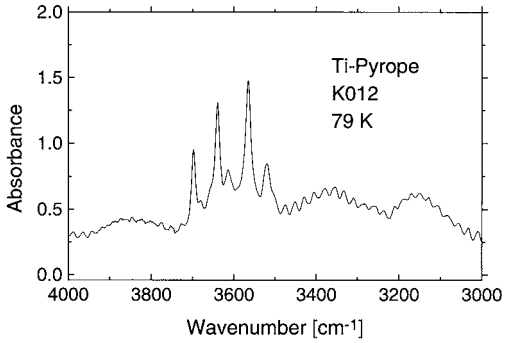

Fig. 10. MIR spectrum of Ti^{4+}-bearing pyrope K012 at 79 K.

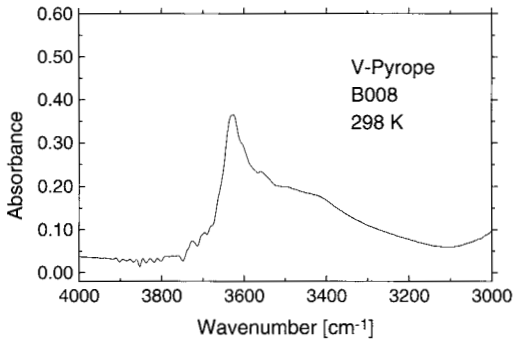

Fig. 11. MIR spectrum of V-bearing pyrope B008 at 298 K.

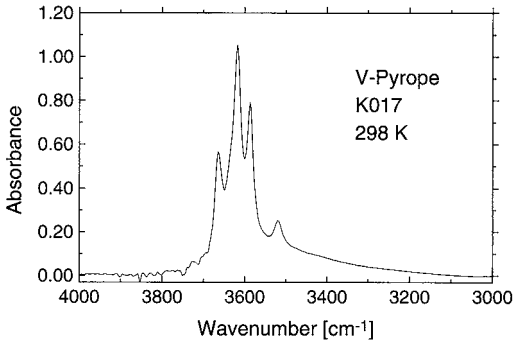

Fig. 12. MIR spectrum of V-bearing pyrope K017 at 298 K.

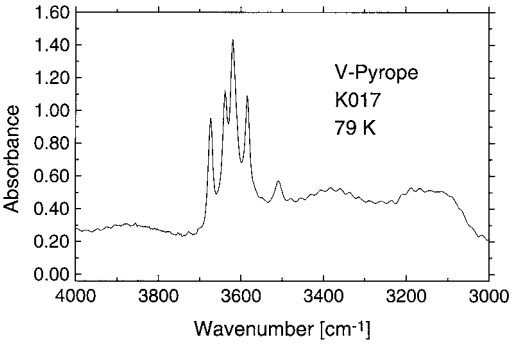

Fig. 13. MIR spectrum of V^{4+}-bearing pyrope K017 at 79 K.

approximately 3686, 3630, 3568 and 3527 cm^{-1} in the room-temperature spectra (Fig. 9). The band at 3630 cm^{-1} splits at 79 K into two bands located at 3636 and 3614 cm^{-1} (Fig. 10). The spectra of V^{3+}- and V^{4+}-bearing pyropes (*e.g.* B008, K020) show only a single band spectrum (Fig. 11), whereas the spectrum of pyrope K017 shows four absorption bands located at 3663, 3630, 3587 and 3520 cm^{-1} (Fig. 12). As is the case for Ti-pyrope, the band at 3630 cm^{-1} splits into two bands at approximately 3639 and 3619 cm^{-1} at 79 K (Fig. 13). The spectrum of pyrope containing both V and Ti (K021 - no spectrum shown) is most similar to the spectrum of Ti-pyrope.

Some of the MIR spectra show small oscillations, which are caused by interference effects in the doubly-polished crystal platelets. In addition, a broad band centred at 3500-3400 cm^{-1} is present in most spectra. It can be assigned to molecular water which is present in tiny fluid inclusions. These features do not affect the interpretation of the spectra given below.

Discussion

UV/VIS absorption spectra

The UV/VIS spectra and the microprobe data on the Cr-, Ni-, Co-bearing pyropes indicate that

these elements substitute for Al^{3+} or Mg^{2+} in pyrope in a straightforward fashion with garnet stoichiometry being preserved. For the Ti- and V-bearing pyropes the case is more complicated. Our UV/VIS spectra of Ti-pyrope are featureless and thus indicate that essentially all Ti occurs in the four-plus state. The microprobe analyses show that it substitutes for Al on the octahedral site. Spectra of synthetic Ti-pyrope were first measured by Khomenko *et al.* (1994b). They proposed that pyropes containing mainly Ti^{4+}, but also some Ti^{3+}, could be grown from hydrothermal syntheses at high pressure. They based this on the blue colour of their pyrope crystals, containing also blue rutile inclusions, whose spectra were characterised by two absorption bands at 22300 and 16100 cm^{-1} in the VIS region. We find the presence of Ti^{3+} surprising, as did they, considering the fO_2 prevailing in their syntheses. The lowest fO_2's used by them are defined by the iron-wüstite buffer (some experiments were also made under unbuffered conditions). The system Ti-O contains two buffer assemblages Ti_2O_3-Ti_3O_5 and Ti_3O_5-TiO_2, the latter of which is located about 5 to 6 log fO_2 units below Fe-FeO at 1-bar and 1000°C (Ihinger & Stolper, 1986). Since the ΔV's of reaction of solid buffers are not too different, we believe that Ti^{4+} should have been the predominant oxidation state in their experiments *if* chemical equilibrium prevailed. The UV/VIS spectrum they describe could be a result of unobserved microscopic rutile inclusions occurring in the pyrope. Indeed, their crystals are very small and characterised by a high inclusion density of rutile. Since Ti^{3+} is present in the rutile, however, there could also be some present in the pyrope. At any rate, we believe that it is the presence of Ti^{4+} in pyrope which gives rise to the multi-band spectrum in the OH^- stretching region and not Ti^{3+}. The spectra of V-bearing pyropes indicate that octahedral Al is also replaced by V^{4+}. The incorporation of these two elements probably leads to defects or vacancies in the garnet structure.

MIR spectra and OH^- substitution mechanism(s)

The MIR spectra of the transition-metal bearing pyropes, which show one absorption band at room temperature and two at ~79 K, are similar to the spectra of hydrothermally grown end-member pyropes (Ackermann *et al.*, 1983; Geiger *et al.*, 1991; Withers *et al.*, 1998). The absorption bands are assigned to OH^- stretching modes resulting from OH^- occurring in the hydrogarnet substitution. Two OH^- stretching bands are predicted based on a symmetry analysis of a $(OH)_4^{4-}$ tetrahedron (Harmon *et al.*, 1982). The presence of the transition metals Cr^{3+}, Co^{2+} and Ni^{2+} in pyrope do not change the OH^- substitution mechanism from that found in end-member pyrope. It appears that OH^- is not coupled with the incorporation of these cations, because no additional substitution other than the hydrogarnet one can be observed. Furthermore, no strong energy shifts of the OH^--stretching modes, caused by local structural distortions and charge density fluctuations (*e.g.* mixed neighbour dodecahedral sites around the tetrahedral sites as proposed by Aines & Rossman, 1984), were observed. The amount of OH^- given as H_2O (Table 4) is also similar to that in end-member pyrope (Geiger *et al.*, 1991).

The MIR spectrum of Ti-bearing pyrope is more complicated. Khomenko *et al.*, (1994a) describe a spectrum with three OH^- bands located at 3684, 3567 and 3528 cm^{-1} at room temperature. The presence of three bands is not consistent with the hydrogarnet substitution and, therefore, they proposed the following OH^- substitution mechanism:

$$^{[6]}Al^{3+} + {}^{[4]}Si^{4+} + 4O^{2-} = {}^{[6]}Ti^{4+} + [(OH)_3O]^{5-} \quad (A)$$

Here three protons substitute for one Si^{4+} cation instead of four, and are coupled with Ti^{4+} on the octahedral site giving charge compensation. The point symmetry of the $[(OH)_3O]^{5-}$ tetrahedron was assumed to be 1, which would lead to a lifting of the degeneracy found in the $\bar{4}3m$ symmetry of an undistorted SiO_4^{4-} tetrahedron. As a consequence, three OH^--stretching bands should occur. However, we observe in our spectra of Ti^{4+}-pyrope the same three bands plus an additional OH^- band at 3630 cm^{-1} (Fig. 9). This band can also be seen, we believe, in the spectra of Khomenko *et al.* (1994a), but its presence is difficult to ascertain due to its low intensity and the noise in the background. Indeed, our low-temperature spectrum at ~79 K shows clearly a five band spectrum (Fig. 10). Our interpretation is that the band at 3630 cm^{-1} in the 298 K spectrum (which splits into two bands at ~79 K as in the other pyropes) reflects the hydrogarnet substitution. Thus, the presence of the other bands would indicate that an additional OH^--substitution mechanism is operating. OH^- is present in these synthetic Ti-containing pyropes *via* at least two substitutions. It is possible that substitution (A) could be the second mechanism, but there is no one to one correlation between the number of Ti cations per formula unit and OH^- groups. Khomenko *et al.* (1994a) considered this and concluded that there exist such large

uncertainties in the estimations of the water concentrations in garnet that substitution (A) is possible. The estimated water concentrations for Ti^{4+}-bearing pyropes are higher than for pyropes containing divalent or trivalent cations (Table 4). It is proposed that the presence of four-valent cations on the octahedral site in garnet leads to increased incorporation of structural OH^-, because the latter is needed to maintain charge balance.

The MIR spectrum of the V^{4+}-bearing pyrope (K017) also shows four bands at 298 K including one at 3630 cm^{-1}. The other bands occur at 3663, 3587 and 3520 cm^{-1}. The 3630 cm^{-1} band splits at ~79 K into two as in the case of Ti-containing pyrope (Fig. 13). Here, however, a different intensity relationship between the bands at 3639 and 3619 cm^{-1} is present. We believe that the incorporation of V^{4+} in pyrope is largely octahedral as is the case for Ti^{4+} and, hence, the OH^- substitution mechanisms and OH^- concentrations in both types of pyropes are similar. In contrast, the spectra of other V-bearing pyropes (B008 and K020) are the same as that of end-member pyrope. The reasons for this are not clear, because it is assumed that all V-bearing pyropes contain both V^{3+} and V^{4+}. The difference between the spectra of garnets B008, K020 and K017 can not be related to the total amount of V, because sample K017 and K020 have similar compositions (Table 3). We propose that varying V^{3+}/V^{4+} ratios are responsible for the different IR spectra. The MIR spectrum of pyrope which contains both V^{4+} and Ti^{4+} is similar to the spectra of Ti-bearing pyrope. No additional or fewer bands are observed.

Geiger *et al.* (1991) observed a multiband MIR spectrum for end-member pyrope synthesised from a gel. The energies of the different OH^- bands are not the same as those of the Ti- and V-bearing pyropes measured herein, but their placements are somewhat similar. Hence, it is possible that the OH^--substitutional mechanisms are similar.

Conclusions and geological implications

The MIR spectra of most natural high-pressure pyrope-rich garnets have fewer OH^- bands than both synthetic pyropes containing 4+ cations and natural grossular-rich garnets, but they are more complicated than synthetics containing 3+ and 2+ transition metals. Natural pyrope-rich garnets are generally characterised by spectra with less than 3 to 4 OH^- bands (Aines & Rossman, 1984; Bell & Rossman, 1992a; Matsyuk *et al.*, 1998). Spectra of natural grossulars are much more complicated and often show multi-band MIR spectra (Rossman & Aines, 1991). The simplest interpretation is that the substitution mechanisms of OH^- in garnet, in general, are largely a function of temperature of crystallisation and/or defect concentrations (*e.g.* grossular-rich garnets crystallise in low-temperature environments compared to pyrope-rich compositions). In the case of synthetic pyrope the OH^- substitutional mechanism(s) and OH^- concentrations do not appear to be directly coupled with the presence of the most common divalent and trivalent cations which are typically found in natural pyrope-rich garnets, when they substitute on the dodecahedral and octahedral site, respectively. In synthetics, as well as in natural pyropes (Bell & Rossman, 1992a), more OH^- can be incorporated in Ti-bearing garnets. However, it is not clear why natural pyropes, which normally have measurable TiO_2 contents, have fewer OH^- bands than Ti-bearing synthetics. In the case of natural pyropes it is difficult to separate out the effects of the physical conditions of crystallisation versus composition in terms of the incorporation of OH^-. That is, natural Ti-bearing pyropes may simply grow in more chemically evolved and water-rich environments than those poorer in Ti.

The results of this study clearly show that the incorporation of highly charged elements, which change the normal mineral stoichiometry, probably by creating vacancies and/or defects, allow additional OH^--substitutional mechanisms and greater OH^- concentrations to be achieved. Similar behaviour has been observed in the case of olivine $(Mg, Fe^{2+})_2SiO_4$ when Fe^{3+} is incorporated (Mackwell & Kohlstedt, 1990).

Synthetic pyropes, without tetravalent cations, show a single band at 3630 cm^{-1} at 298 K and a two-band spectrum at ~79 K (Geiger *et al.*, 1991; this work). The incorporation of small amounts of Cr_2O_3 or NiO does not appear to affect the wavenumber of the absorption bands, nor does it increase their number. Synthetic almandine shows two bands at 298 K (3613 and 3490 cm^{-1}) and ~79 K (3617 and 3592 cm^{-1}) (Geiger *et al.*, 1989). If these two synthetic garnets are characterised by the hydrogarnet substitution, which is the most logical assumption, then we should expect natural high-pressure pyrope-rich garnets, which consist mostly of pyrope and almandine components, to show a strong OH^- absorption band around 3625 cm^{-1} at 298 K. Most, however, do not show this. Most natural mantle pyropes are characterised by spectra with OH^- absorption bands located between 3645-3662 cm^{-1} and 3561-3583 cm^{-1}

(Matsyuk *et al.*, 1998; Bell & Rossman, 1992a) and, hence, would not appear to be characterised by the hydrogarnet substitution. A small class of pyrope-rich garnets belonging to the so-called "Ca group" are, though, characterised by an OH^- band located at 3623-3631 cm^{-1} (Matsyuk *et al.*, 1998) and they are the best candidates for having the classic hydrogarnet substitution. Such garnets come from grospydite parageneses or are from corundum-bearing eclogites. Indeed, Beran *et al.* (1993) describe a grossular-rich garnet from a grospydite xenolith having a single band at 3630 cm^{-1}. This garnet is relatively H_2O rich containing about 0.062 wt. % H_2O. Thus the OH^-–substitution mechanism and the OH^- concentrations are similar to the synthetic pyropes. Other pyrope-rich garnets from "normal" mantle garnet peridotites, however, would appear to have OH^-–substitution(s) different from the hydrogarnet one. In addition, these contain much less H_2O. This difference is related to the lower f_{H_2O} prevailing during the growth of the the natural pyropes compared to the synthetics. The similarities between synthetic pyropes and garnets in grospydites indicate high water fugacities in their formation. This is consistent with the idea that grospydites result from the metamorphism of rodingites.

Acknowledgements: We would like to thank Andreas Fehler for sample preparation and Drs. S. Matsyuk and V. M. Khomenko for their reviews of a first draft of the manuscript. Drs. M. Andrut and M. Wildner are also thanked for their formal reviews which helped to clarify several points. This work was supported in part by the National Science Foundation (USA) grant EAR-9804871.

References

Ackermann, L., Cemič, L., Langer, K. (1983): Hydrogarnet substitution in pyrope: a possible location for "water" in the mantle. *Earth Planet. Sci. Lett.*, **62**, 208-214.

Aines, R.D. & Rossman, G.R. (1984): Water content of mantle garnets. *Geology*, **12**, 720-723.

Amthauer, G. (1976): Kristallchemie und Farbe chromhaltiger Granate. *N. Jb. Mineral. Abh.*, **126**, 158-186.

Armbruster, T., Birrer, J., Libowitzky, E., Beran, A. (1998): Crystal-chemistry of Ti-bearing andradites. *Eur. J. Mineral.*, **10**, 907-921.

Basso, R., Cimmino, F., Messiga, B. (1984): Crystal chemistry of hydrogarnets from three different microstructural sites of a basaltic metarodingite from the Voltri Massif (Western Liguria, Italy). *N. Jb. Mineral. Abh.*, **148**, 246-258.

Bell, D.R. & Rossman, G.R. (1992a): The hydrous component in garnets from the subcontinental mantle of southern Africa. *Contrib. Mineral. Petrol.*, **111**, 161-178.

—, — (1992b): Water in Earth's mantle: the role of nominally anhydrous minerals. *Science*, **255**, 1391-1397.

Beran, A., Langer, K., Andrut, M. (1993): Single crystal infrared spectra in the range of OH fundamentals of paragenetic garnet, omphacite and kyanite in an eclogitic mantle xenolith. *Mineral. Petrol.*, **48**, 257-268.

Burns, R.G. (1993): Mineralogical Applications of Crystal Field Theory, 2. edition. Putnis ed., Cambridge, 551 p.

Cemič, L., Geiger, C.A., Hoyer, W.W., Koch-Müller, M., Langer, K. (1990): Piston-cylinder techniques: Pressure and temperature calibration of a pyrophyllite-based assembly by means of DTA measurements, a salt-based assembly, and a cold sealing sample encapsulation method. *N. Jb. Mineral. Mh.*, **1990/2**, 49-64.

Cho, H. & Rossman, G.R. (1993): Single-crystal NMR studies of low-concentration hydrous species in minerals: Grossular garnet. *Am. Mineral.*, **78**, 1149-1164.

Cohen-Addad, C., Ducros, P., Bertaut, E.F. (1967): Etude de la substitution du groupement SiO_4 par $(OH)_4$ dans les composés $Al_2Ca_3(OH)_{12}$ et $Al_2Ca_3(SiO_4)_{2.16}(OH)_{3.36}$ de type grenat. *Acta Cryst.*, **23**, 220-230.

Geiger, C.A., Lager, G.A., Amthauer, G., Richardson, J.K, Armbruster, T. (1989): Almandine garnet: synthesis, structure, and Mössbauer and NIR spectroscopy. XII European Crystallographic Meeting, Moscow, USSR, Collected Abstracts, **2**, 6.

Geiger, C.A., Langer, K., Bell, D.R., Rossman, G.R., Winkler, B. (1991): The hydroxide component in synthetic pyrope. *Am. Mineral.*, **76**, 49-59.

Harmon, K.M., Gabriele, J.M., Nuttal, A.S. (1982): Hydrogen bonding in the tetrahedral $O_4H_4^{4-}$ cluster in hydrogrossular. *J. Mol. Structure*, **82**, 213-219.

Ihinger, P.D. & Stolper, E. (1986): The color of meteoritic hibonite: an indicator of oxygen fugacity. *Earth Planet. Sci. Lett.*, **78**, 67-79.

Khomenko, V.M., Langer, K., Beran, A., Koch-Müller, M., Fehr, T. (1994a): Titanium substitution and OH-bearing defects in hydrothermally grown pyrope crystals. *Phys. Chem. Minerals*, **20**, 483-488.

Khomenko, V.M., Langer, K., Andrut, M., Koch-Müller, M., Vishnevsky, A.A. (1994b): Single crystal absorption spectra of synthetic Ti, Fe-substituted pyropes. *Phys. Chem. Minerals.*, **21**, 434-440.

Lager, G.A., Armbruster, T., Rotella, F.J., Rossman, G.R. (1989): OH-substitution in garnets: X-ray and neutron diffraction, infrared, and geometric-modeling studies. *Am. Mineral.*, **74**, 840-851.

Mackwell, S.J. & Kohlstedt, D.L. (1990): Diffusion of hydrogen in olivine: implications for water in the mantle. *J. Geophys. Res.*, **95**, 5079-5088.

Manning, P.G. & Harris, D.C. (1970): Optical-absorption and electron-microprobe studies of some high-Ti andradites. *Can. Mineral.*, **10**, 260-271.

Martin, R.F. & Donnay, G. (1972): Hydroxyl in the mantle. *Am. Mineral.*, **57**, 554-570.

Matsyuk, S.S., Langer, K., Hösch, A. (1998): Hydroxyl defects in garnets from mantle xenoliths in kimberlites of the Siberian platform. *Contrib. Mineral. Petrol.*, **132**, 163-179.

Reid, A.M., Brown, R.W., Dawson, J.B., Whithefield, G.G. (1976): Garnet and pyroxene compositions in some diamondiferous eclogites. *Contrib. Mineral. Petrol.*, **58**, 203-220.

Ross II, C.R., Keppler, H., Canil, D., O'Neill, H.St.C. (1996): Structure and crystal-field spectra of $Co_3Al_2(SiO_4)_3$ and $(Mg,Ni)_3Al_2(SiO_4)_3$ garnet. *Am. Mineral.*, **81**, 61-66.

Rossman, G.R. & Aines, R.D. (1991): The hydrous components in garnets: Grossular-hydrogrossular. *Am. Mineral.*, **76**, 1153-1164.

Rossman, G.R., Beran, A., Langer, K. (1989): The hydrous component of pyrope from the Dora Maira Massif, Western Alps. *Eur. J. Mineral.*, **1**, 151-154.

Schmetzer, K. & Ottemann, J. (1979): Kristallchemie und Farbe Vanadium-haltiger Granate. *N. Jb. Mineral. Abh.*, **136**, 146-168.

Tanabe, Y. & Sugano, S. (1954): On the absorption spectra of complex ions I, II. *J. Phys. Soc. Japan*, **9**, 753-779.

Weber, M.J. & Riseberg, L.A. (1971): Optical spectra of vanadium ions in yttrium aluminum garnet. *J. Chem. Phys.*, **55**, 2032-2038.

Wilkins, R.W.T. & Sabine, W. (1973): Water content of some nominally anhydrous silicates. *Am. Mineral.*, **58**, 508-516.

Withers, A.C., Wood, B.J., Carroll, M.R. (1998): The OH content of pyrope at high pressure. *Chemical Geol.*, **147**, 161-171.

Received 4 May 1999
Modified version received 23 August 1999
Accepted 8 October 1999